0026-895X/07/7203-734–743$20.00
MOLECULAR PHARMACOLOGY
Copyright © 2007 The American Society for Pharmacology and Experimental Therapeutics
Mol Pharmacol 72:734–743, 2007

Vol. 72, No. 3
35550/3246231
Printed in U.S.A.

Functional Characterization of the Promoter of Human Carbonyl Reductase 1 (*CBR1*). Role of *XRE* Elements in Mediating the Induction of *CBR1* by Ligands of the Aryl Hydrocarbon Receptor

Sukhwinder S. Lakhman, Xiaomin Chen, Vanessa Gonzalez-Covarrubias, Erin G. Schuetz, and Javier G. Blanco

Department of Pharmaceutical Sciences, the State University of New York at Buffalo, Buffalo, New York (S.S.L., X.C., V.G.-C., J.G.B.); Department of Pharmaceutical Sciences, St. Jude Children Research Hospital, Memphis, Tennessee (E.G.S.)

Received February 26, 2007; accepted June 14, 2007

ABSTRACT

Human carbonyl reductase 1 (CBR1) metabolizes a variety of substrates, including the anticancer doxorubicin and the antipsychotic haloperidol. The transcriptional regulation of *CBR1* has been largely unexplored. Therefore, we first investigated the promoter activities of progressive gene-reporter constructs encompassing up to 2.4 kilobases upstream of the translation start site of *CBR1*. Next, we investigated whether *CBR1* mRNA levels were altered in cells incubated with prototypical receptor activators (e.g., dexamethasone and rifampicin). *CBR1* mRNA levels were significantly induced (5-fold) by the ligand of the aryl hydrocarbon receptor (AHR) β-naphthoflavone. DNA sequence analysis revealed two xenobiotic response elements ($_{-122}$*XRE* and $_{-5783}$*XRE*) with potential regulatory functions. *CBR1* promoter constructs lacking the $_{-122}$*XRE* showed diminished (9-fold) promoter activity in AHR-proficient cells incubated with β-naphthoflavone. Fusion of $_{-5783}$*XRE* to the $_{-2485}$*CBR1* reporter construct enhanced its promoter activity after incubations with β-naphthoflavone by 5-fold. Furthermore, we tested whether the potent AHR ligand 2,3,7,8-tetrachlorodibenzo-*p*-dioxin (TCDD) induced *Cbr1* expression in *Ahr*$^{+/-}$ and *Ahr*$^{-/-}$ mice. TCDD induced hepatic *Cbr1* mRNA (TCDD, 2-fold) and *Cbr1* protein levels (TCDD, 2-fold) in *Ahr*$^{+/-}$ mice compared with vehicle-injected controls. In contrast, no significant *Cbr1* mRNA and Cbr1 protein induction was detected in livers from *Ahr*$^{-/-}$ mice treated with TCDD. These studies provide the first insights on the functional characteristics of the human *CBR1* gene promoter. Our data indicate that the AHR pathway contributes to the transcriptional regulation of *CBR1.*

Human carbonyl reductase 1 (CBR1) catalyzes the NADPH-dependent reduction of a variety of xenobiotic compounds including smoke derived carcinogens and many relevant pharmacological agents. For example, CBR1 catalyzes the two-electron reduction of the C-13 carbonyl group of the anticancer anthracyclines doxorubicin and daunorubicin to generate their corresponding alcohol metabolites (doxorubicinol and daunorubicinol) (Forrest and Gonzalez, 2000). Anthracycline C-13 alcohol metabolites are cardiotoxic, have diminished tumor cell killing activities, circulate in plasma at various levels, and contribute to the unpredictable pharmacology of anthracycline drugs (Frost et al., 2002; Minotti et al., 2004). Significant interindividual variability in carbonyl reductase activity (CBR) has been documented in liver, erythrocytes, and in breast and lung tumors (Iwata et al., 1993; Wong et al., 1993; Rady-Pentek et al., 1997; Lopez de Cerain et al., 1999). We observed wide ranges of CBR activities in liver cytosols from black (range, 4.1–21.5 nmol/min · mg) and white donors (range, <0.1–28.0 nmol/min · mg) (Covarrubias et al., 2006). However, the molecular basis of such disparities and its potential impact on CBR-mediated drug metabolism remain to be elucidated. We hypothesize that interindividual differences in CBR activity may in part

This work was supported by National Institutes of Health/National Institute of General Medical Sciences grant R01-GM73646 (to J.G.B.) and National Institutes of Health/National Institute of General Medical Sciences grant R01-GM60346 (to E.G.S.).
Article, publication date, and citation information can be found at http://molpharm.aspetjournals.org.
doi:10.1124/mol.107.035550.

ABBREVIATIONS: CBR1, human carbonyl reductase 1; AHR, aryl hydrocarbon receptor; CBR, carbonyl reductase activity; XRE, xenobiotic response element; TCDD, 2,3,7,8-tetrachlorodibenzo-*p*-dioxin; TCPOBOP, 1,4-bis-[2-(3,5-dichloropyridyloxy)]-benzene; kb, kilobase; bp, base pair; PCR, polymerase chain reaction; ANOVA, analysis of variance; RT-PCR, reverse transcription-polymerase chain reaction; DMSO, dimethyl sulfoxide; GAPDH, glyceraldehyde-3-phosphate dehydrogenase; DBTSS, Data Base of Transcriptional Start Sites; SP1, specificity protein 1; NNK, 4-methylnitrosamino-1-(3-pyridyl)-1-butanone; BP, benzo(*a*)pyrene.

reflect variable rates of *CBR1* gene transcription. *CBR1* spans approximately 3.2 kb on chromosome 21 (21q22.13), contains three exons, and encodes for a monomeric 277 amino acid protein with a molecular weight of 30,375 (Wermuth et al., 1988). It is noteworthy that despite the major role of CBR1 in the biotransformation of xenobiotics, there is a paucity of reports focused on the functional characterization of the human *CBR1* gene promoter. Therefore, the first aim of our study was to investigate the potential promoter activities of progressive DNA deletion constructs encompassing up to 2485 base pairs (bp) of genomic sequence 5′ upstream the translation start site of *CBR1* by using gene-reporter assays.

Our second aim was to test whether *CBR1* mRNA levels were induced in cell cultures incubated with prototypical activators of the nuclear glucocorticoid receptor, the constitutive androstane receptor, the pregnane X receptor, and the aryl hydrocarbon receptor (AHR), respectively. We detected significant induction of *CBR1* mRNA expression in HepG2 and MCF-7 cells treated with the AHR ligand β-naphthoflavone. AHR is a ligand-activated basic helix-loop-helix transcription factor that participates in the regulation of several key mammalian genes involved in the metabolism of xenobiotics (e.g., *CYP1A1* and *CYP1B1*). After ligand binding, AHR translocates from the cytoplasm into the nucleus to form a complex with aryl hydrocarbon receptor nuclear translocator. The resulting ligand/AHR/aryl hydrocarbon receptor nuclear translocator complex interacts with specific DNA sequences termed xenobiotic responsive elements (*XRE*s) to induce the transcription of target genes (Nebert et al., 2000; Nioi and Hayes, 2004). The consensus *XRE* sequence (5′-$^{T}/_{G}$NGCGTG-3′) contains the substitution intolerant *XRE* core motif (5′-GCGTG-3′) (Lusska et al., 1993). It is interesting that we identified two perfect *XRE* motifs located at 122 bp and 5783 bp upstream the translation start site of *CBR1* ($_{-122}$*XRE*, and $_{-5783}$*XRE*). Therefore, our third aim was to investigate the functional impact of the proximal ($_{-122}$*XRE*), and distal ($_{-5783}$*XRE*) *XRE* motifs by performing gene reporter assays with engineered *CBR1* promoter constructs.

The development of *Ahr*-deficient mice (*Ahr*$^{-/-}$) has contributed to the identification of a battery of genes regulated through the AHR pathway (Fernandez-Salguero et al., 1995; Zaher et al., 1998; Sugihara et al., 2001; Jiang et al., 2004). AHR mediates the induction of several key xenobiotic-metabolizing enzymes such as CYP1A1, CYP1B1, glutathione transferase, and NAD(P)H:quinone oxidoreductase (NQO1) (Nebert et al., 2000; Shimada et al., 2002). Thus, we extended our observations by testing whether the potent AHR ligand 2,3,7,8-tetrachlorodibenzo-p-dioxin (TCDD) induced *Cbr1* mRNA and Cbr1 protein levels in livers from *Ahr*-proficient (*Ahr*$^{+/-}$), and *Ahr*-deficient (*Ahr*$^{-/-}$) mice. Together, our findings provide insights on the regulation of *CBR1* and lay the foundation for future studies aimed toward the elucidation of the molecular bases that govern variable CBR activity in humans.

Materials and Methods

Cell Culture and Reagents. HepG2 (human hepatocarcinoma, HB-8065), and MCF-7 (human breast adenocarcinoma, HTB-22) cell lines were obtained from the American Type Culture Collection (Manassas, VA). Minimum essential medium, fetal bovine serum, and other cell culture reagents were purchased from Invitrogen (Carlsbad, CA). Cells were routinely cultured in 75-cm^2 vented flasks using α-minimum essential medium supplemented with 10% fetal bovine serum. Cultures were grown in an incubator at 37°C, 5% CO_2, and 95% relative humidity. Cultures were maintained at low passage numbers (n <12) and were free of mycoplasma contamination.

Dexamethasone, clotrimazole, 1,4-bis-[2-(3,5-dichloropyridyloxy)]-benzene (TCPOBOP), and rifampicin were purchased from Sigma-Aldrich (St. Louis, MO). β-Naphthoflavone was purchased from Indofine (Hillsborough, NJ).

Cloning of *CBR1* Promoter Constructs. Approximately 5 kilobases of DNA sequence upstream from the translation start codon (ATG) of *CBR1* were amplified from human DNA sample HD17030 (Coriell Institute for Medical Research, Camden, NJ) by using the Expand Long Template PCR system (Roche, Indianapolis, IN). PCR primers were 5′-CCCCTGACTGCCCTTTCTTA-3′ (forward) and 5′-TCACCAGCGCTACATGGAT-3′ (reverse). A derivative fragment of 2485 bp was cloned into a pGL3 basic luciferase vector (Promega, Fitchburg, WI) by using the following primers: 5′-GCTCTTACGCGTGCTAGCCCGAGCTCTGAATTATCCTGAGTGG-3′ (forward), and 5′-CCGCGCGCCCCGTTCAGCCGAATTCATCTGCGATCTAAG-3 (reverse). Eight 5′ progressive deletion constructs were made by PCR using primers listed below. The resulting products were cloned into pGL3 basic firefly luciferase reporter vectors. The identity of each construct and the absence of cloning artifacts were verified by direct sequencing with the dye-terminator method in a 3130XL Genetic Analyzer (Applied Biosystems, Foster City, CA).

The $_{-122}$*XRE* substitution intolerant core (5′-GCGTG-3′) was deleted from the $_{-413}$*CBR1* promoter construct using the QuikChange site-directed mutagenesis kit (Stratagene, La Jolla, CA) with the following primers: 5′-CCTGCGCGCTCAGCGGCCGGTAACCCACGGGTGCGCGCCC-3′, and 5′-GGGCGCGCACCCGTGGGTTACCGGCCGCTGAGCGCGCAGG-3′. Deletion of $_{-122}$*XRE* was confirmed by direct sequencing analysis.

A 12-bp sequence containing the distal $_{-5783}$*XRE* element (5′-TTGCGTGCCTTG-3′, bases −5790 to −5779) was added to the 5′ end of the $_{-2485}$*CBR1* construct by using QuikChange with the following primers: 5′-CGCGTGCTAGCCTTGCGTGCCTTGGAGCTCTGAATTATCC-3′, and 5′-GGATAATTCAGAGCTCCAAGGCACGCAAGGGCTAGCACGCG-3′. The addition of $_{-5783}$*XRE* was verified by direct sequencing.

List of primers. The forward primers included $_{-1847}$*CBR1*: 5′-CCTAAATCTGTACTGCCCAATACGCGTACAGTGACCACTAACACATGC-3′; $_{-1561}$*CBR1*: 5′-GAGGGAGTCACTCTGTTGACGCGTCCCAGGCTGGAGTGCAG-3′; $_{-1101}$*CBR1*: 5′-CCAGACCCCTCACCTGCAACGCGTGCCTGATGCCTGTTGAC-3′; $_{-746}$*CBR1*: 5′-GGTACATCCTAGAGTGTACGCGTTATTGTCCGTGTAAAATAGGG-3′; $_{-600}$*CBR1*: 5′-CTGGCTAAGTCAGTAGCACGCGTTTTGTTTTCATATACTTAGGGG-3′; $_{-413}$*CBR1*: 5′-CACAACTAGGAATGA*ACGCGT*TTGAACAGCTGGGAG-3′; $_{-205}$*CBR1*: 5′-GCTCCGCACCCCGGACGCGTGGTTCCGGTGG-3′; and $_{-101}$*CBR1*: 5′-GGGCGTGTAACCCACGCGTGCGCGCCCACG-3′; The reverse primer was $_{Rev}$*CBR1*: 5′-CCGCGCGCCCCGTTCAGCCGAATTCATCTGCGATCTAAG-3′.

Transient Transfections and Luciferase Activity Assays. Cells were plated 24 to 48 h before transfections in 12-well plates. Reporter gene constructs (firefly luciferase) and the SV40-driven *Renilla reniformis* luciferase pRL-SV40 plasmid (Promega) were cotransfected into 60 to 70% confluent cell cultures by using FuGENE 6 (Roche). Twenty-four hours after cotransfection, cultures were washed once with phosphate-buffered saline solution, and the cells were lysed with passive lysis buffer (250 μl/well) (Promega). Cell lysates were incubated at room temperature (15 min), mixed with a vortex blender (10 s), and centrifuged at 4°C (1500 rpm for 30 s). Luciferase reporter gene activities were determined with the Dual-Luciferase Reporter Assay System (Promega) according to the manufacturer's instructions. Light intensity was measured in a Synergy HT luminometer equipped with proprietary software for data analysis (BioTek, Winooski, VT). Light intensity values from cell cultures

transfected with the promoterless (pGL3) vector were used to correct for background. Corrected firefly luciferase activities were normalized to *R. reniformis* luciferase activities and expressed as fold increases with respect to the values obtained with pGL3-basic empty vector. In all cases, three to five independent experiments were performed in duplicate to evaluate reproducibility. Unpaired Student's *t* tests (two groups) and analysis of variance (ANOVA, three or more groups) were used to compare experimental means. In all cases, differences were considered to be significant at $p < 0.05$. Computations were performed with Microsoft Excel 2000 version 9.0 (Microsoft, Redmond, WA) and SigmaPlot version 8.02 (SPSS Inc., Chicago, IL).

Quantification of *CBR1* mRNA in Cell Cultures by Real-Time RT-PCR. Cell cultures (70–80% confluence) were treated for 24 h with dexamethasone (10 μM), rifampicin (10 μM), β-naphthoflavone (10–50 μM), clotrimazole (20 μM), TCPOBOP (0.250 μM), or vehicle (DMSO). Total RNA was extracted with RNeasy Mini kit (QIAGEN, Valencia, CA) according to the manufacturer's instructions. RNA was eluted with molecular biology-grade water, and stored at −80°C until use. RNA concentrations were measured by spectrophotometric analysis at 260 nm in a Shimadzu UV-1601 PC spectrophotometer (Shimadzu, Kyoto, Japan). Total RNA (100 ng) was reverse-transcribed and amplified by using one-step QuantiTect SYBR Green RT-PCR kits (QIAGEN). RT-PCR reaction mixtures were incubated on a MX4000 engine thermal cycler equipped with proprietary software for data analysis (Stratagene). The comparative quantitation method was used to determine relative *CBR1* mRNA levels in drug-treated samples. Vehicle-treated samples were used as references, and individual β-actin mRNA levels were used as normalizers (Blanquicett et al., 2002; Bustin, 2002). *CBR1* primers were: 5′-CTGATCCCACACCCTTTCAT-3′ (forward), and 5′-TTAAGGGCTCTGACGCTCAT-3′ (reverse); β-actin primers, 5′-ACGGCTCCGGCATGTGCAAG-3′ (forward), and 5′-TGACGATGCCGTGCTCGATG-3′ (reverse). Cycling parameters for the amplifications in parallel of *CBR1* and β-actin mRNAs were: 50°C for 30 min (reverse transcription), 95°C for 10 min (*Taq* polymerase activation); 40 cycles of 95°C for 15 s (denaturation), 51°C for 30 s (annealing), 72°C for 30 s (extension), and 78°C for 30 s (fluorescence collection). Standard curves for *CBR1* and β-actin mRNA (10-fold dynamic range) were run in parallel to ensure accurate mRNA quantifications. In all cases, the regression coefficients (r) of the standard curves were $r \geq 0.9$. Amplification efficiencies for *CBR1* and β-actin mRNAs were similar and ranged between 125 and 175%. In all cases, experimental samples and standards for calibration curves were analyzed in quadruplicate.

Animals and Treatments. $Ahr^{+/-}$ and $Ahr^{-/-}$ mice were procured from the laboratory of Dr. Christopher Bradfield (University of Wisconsin). The Institutional Animal Care and Use Committee approved the experimental protocol. Animals were housed in a temperature- and humidity-controlled room under a light cycle with free access to food and water. Mice (aged 81 ± 14 days) were treated with intraperitoneal injections of TCDD (50 μg/kg; AccuStandard Inc., New Haven, CT), or corn oil vehicle (200 μl), respectively. Animals were sacrificed by CO_2 inhalation. Livers were removed, snap-frozen in liquid nitrogen, and stored at −80°C until use.

Quantification of Hepatic *Cbr1* mRNA by Real-Time RT-PCR. Liver RNA was extracted with RNeasy Mini kits (QIAGEN). RNA samples (100 ng) were subjected to one-step quantitative real-time RT-PCR using QuantiTect SYBR green RT-PCR kit (QIAGEN). Mouse *Cbr1* primers were: 5′-ATCACTCGTGACCTGTGTCG-3′ (forward), and 5′-GGTGTCGTCATTGACCTTGA-3′(reverse); β-actin primers: 5′-GACCCAGATCATGTTTGAGACCTTC-3′ (forward), and 5′-GGAGTCCATCACAATGCCAGTG-3′ (reverse). Amplification conditions for murine *Cbr1* and β-actin mRNAs were: 50°C for 30 min (reverse transcription), 95°C for 10 min (*Taq* polymerase activation); 40 cycles of 95°C for 15 s (denaturation), 52°C for 30 s (annealing), 72°C for 30 s (extension), and 78°C for 30 s (fluorescence collection). Standard curves (10-fold dynamic range) for *Cbr1* and β-actin mRNA were run in parallel. Relative *Cbr1* mRNA levels were calculated by using the comparative quantitation method as described above. Samples were analyzed in quadruplicate.

Detection of Hepatic Cbr1 by Immunoblotting. Fragments of frozen mouse liver were homogenized in three volumes of ice-cold lysis buffer (Promega). The homogenates were centrifuged at 13,000*g* for 20 min at 4°C. The resulting supernatants (100 μg) were separated on 4 to 20% precast polyacrylamide gels (Pierce, Rockford, IL) and transferred onto Hybond ECL nitrocellulose membranes (GE Healthcare, Chalfont St. Giles, Buckinghamshire, UK). Membranes were first incubated with a monoclonal anti-human CBR1 antibody (1:1000 dilution) that cross-react with murine Cbr1 (Abnova Corporation, Taipei City, Taiwan) and with a secondary anti-mouse IgG conjugated with horseradish peroxidase (1:1000 dilution; GE Healthcare). The membranes were also probed with anti-glyceraldehyde-3-phosphate dehydrogenase (GAPDH) antibody (1:10,000 dilution; Chemicon International, Temecula, CA) to correct for differences in protein loading. Immunoreactive bands were visualized with the ECL Plus Western blotting detection system (GE Healthcare) and quantified by using a ChemiDoc XRS gel documentation system equipped with Quantity One software (Bio-Rad Laboratories, Hercules, CA).

CBR Activity. Maximal CBR activity was measured in cellular lysates, and in mice liver cytosols by using the specific NQO1 inhibitor dicoumarol in the presence of the substrate menadione and the NADPH cofactor (Wermuth et al., 1986; Bello et al., 2004; Covarrubias et al., 2006). Typical incubation mixtures (1 ml) contained sodium phosphate buffer (0.1 M), pH 7.4, 200 μM NADPH (Sigma-Aldrich), 200 μM menadione (Sigma-Aldrich), and 5 μM dicoumarol. Mixtures were equilibrated for 2 min at 37°C after the addition of cytosols (200 μg). The rates of NADPH oxidation were recorded for 4 min at 37°C in a Cary Varian Bio 300 UV-visible spectrophotometer (Palo Alto, CA). Enzymatic velocities were automatically calculated by linear regression of the $\Delta_{abs}/\Delta_{time}$ points (2400 readings) and expressed as micromoles per minutes per milligram. Protein concentrations were determined with the Bradford assay (Bio-Rad).

Results

Cloning and Functional Analysis of *CBR1* Promoter Constructs. First, we cloned a 2485-bp DNA fragment from the 5′-flanking region of *CBR1* to perform functional characterization studies. Sequencing of the insert revealed 100% identity with a segment of nucleotide sequence from locus AP001724 (*Homo sapiens* genomic DNA, chromosome 21q, section 68/105; Entrez Nucleotide Database, available at http://www.ncbi.nlm.nih.gov/sites/entrez?db=Nucleotide). According to the Data Base of Transcriptional Start Sites (DBTSS), *CBR1* has a predominant transcription start site (TSS, 123/146 cDNA clones) located 92 bp upstream of the ATG codon (Fig. 1). Analysis of the core promoter sequence of *CBR1* revealed the presence of a typical initiator element containing the TSS [Inr, Py-Py(C)-A_{+1}-N-T/A-Py-Py]. The *CBR1* core promoter region has no downstream core promoter element (A/G_{+28}-G-A/T-C/T-G/A/C), no TATA box, and no CAAT box. The core promoter is embedded in a CpG island of approximately 0.65 kb that encompasses −273 bp of 5′-flanking sequence, and extends 369 bp downstream of the ATG codon. There are two contiguous GC boxes located at −165 and −152 bp, respectively. In addition, there is a proximal SP1 motif at −53 bp and a relatively more distal SP1 motif embedded in the −152 bp GC box. Together, these findings indicate that the core promoter of *CBR1* has the configuration of a typical CpG island promoter (Butler and Kadonaga, 2002).

Computer-assisted searches for additional *cis*-acting elements using the TESS and TRANSFAC databases pinpointed potential consensus motifs for a number of transcription factors including hepatic nuclear factor-3β, Ikaros 2 protein, and octamer-binding transcription factor (Fig. 1). We identified one proximal sequence motif for a xenobiotic response element ($_{-122}$*XRE*; Fig. 1). Further analysis of up to 6 kb upstream of the ATG codon revealed a distal *XRE* motif containing the substitution-intolerant core sequence 5′-GCGTG-3′ at position −5783 ($_{-5783}$*XRE*).

Next, we generated a series of progressive 5′-deletion constructs and performed gene reporter assays in HepG2 and MCF-7 cells (Fig. 2, A and B). Results from both cell lines suggested the presence of a negative regulatory element in the −2485/−1847 region, because deletion of the 653-bp segment resulted in significant increases in luciferase activities (HepG2, Student's t test, $p < 0.05$; MCF-7, Student's t test, $p < 0.05$). In both cell lines, further 5′ truncation of up to 746 bp resulted in no significant changes in the promoter activities of constructs $_{-1847}$*CBR1*, $_{-1561}$*CBR1*, and $_{-1101}$*CBR1,* respectively (HepG2, ANOVA, $p = 0.75$; MCF-7, ANOVA, $p = 0.83$). In HepG2 cells, the $_{-413}$*CBR1* construct exerted the highest promoter activity from the series suggesting that the −600/−413 region may harbor an element whose regulatory role depends on the cellular context. Further deletion of 208 bp ($_{-205}$*CBR1*) decreased the promoter activity in HepG2 (2.7-fold) and MCF-7 cells (2.4-fold). Data from both cell lines showed that the −205/−101 region contains *cis*-acting elements that are crucial to sustain gene transcription because deletion of 104 bp resulted in substantial decreases in the promoter activities by 22-fold (HepG2, Student's t test, $p < 0.01$) and 41-fold (MCF-7, Student's t test, $p < 0.001$), respectively. The −205/−101 segment contains two GC boxes and the proximal $_{-122}$*XRE.* Thus, it is likely that the removal of these elements resulted in a construct ($_{-101}$*CBR1*) with diminished promoter activity (Figs. 1 and 2). In both cell lines, the $_{-101}$*CBR1* showed minimal although significant increases in transcriptional activity compared with the pGL3-Basic vector (HepG2 = 3-fold, Student's t test, $p < 0.05$; MCF-

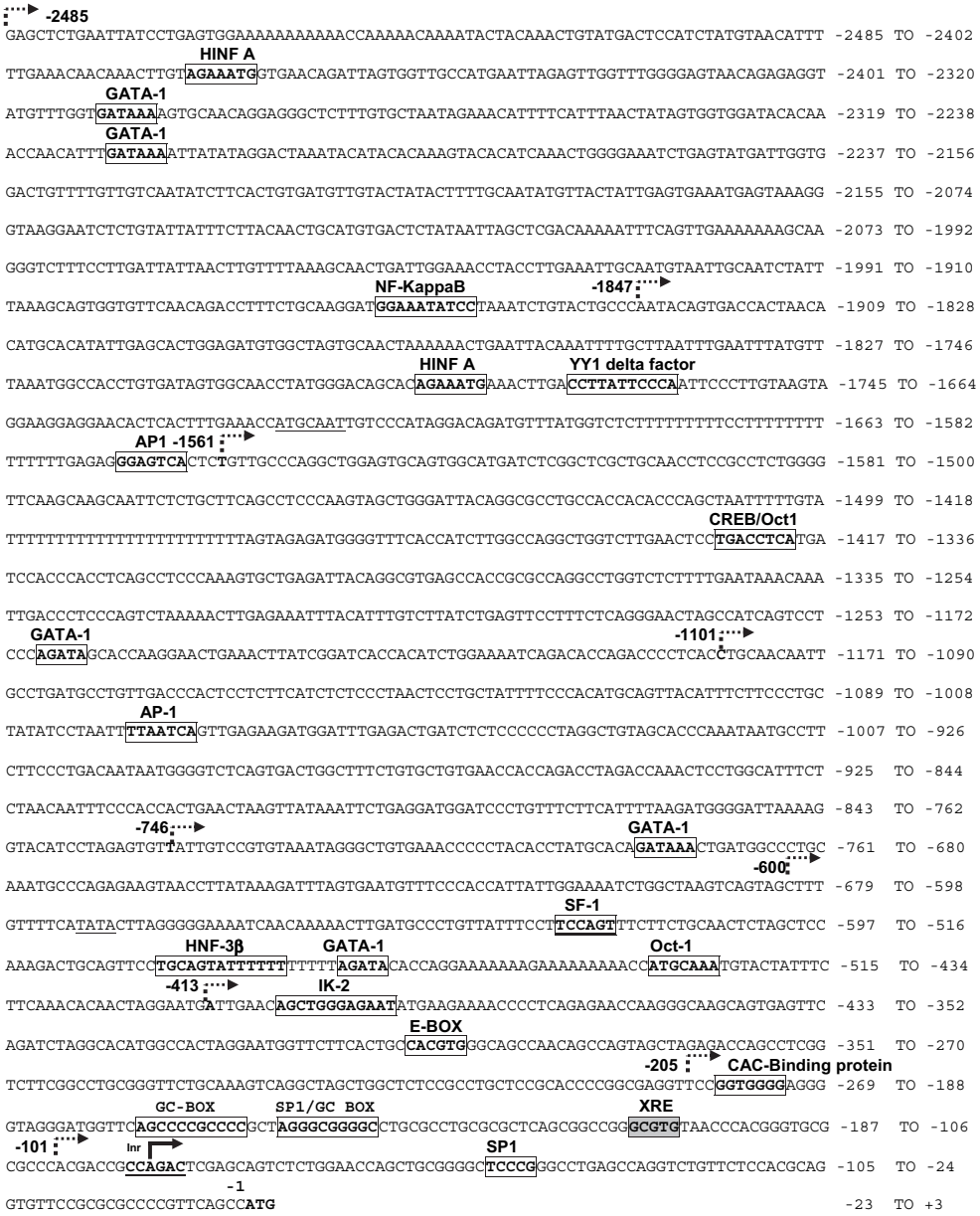

Fig. 1. Annotated sequence from the 5′-flanking region of human *CBR1*. The transcription start site (−92 bp, DBTSS) is indicated with a solid arrow, and the Inr element is underlined. The different fragments corresponding to the series of deletion promoter constructs are indicated with dotted arrows. The proximal *XRE* motif ($_{-122}$*XRE*) is indicated in a gray box, and putative transcription factor binding sites are indicated in clear boxes. AP1, activator protein 1; HINF A, histone nuclear factor A; SF1, steroidogenic factor 1; NF-κB, nuclear factor κ B; Oct 1, octamer-binding transcription factor; CAC, CACCC binding protein; IK-2, Ikaros 2 protein; GATA, GATA or GATAA sequence; HNF 3β, hepatic nuclear factor 3β; YY1, Yin Yang 1.

7 = 8-fold, Student's t test, $p < 0.05$). It is possible that the Inr element (−93 bp) and the proximal SP1 site (−53 bp) dictate the minimal promoter activity of the $_{-101}$*CBR1* construct.

Induction of *CBR1* mRNA and CBR Activity by a Ligand of the Aryl Hydrocarbon Receptor. To pinpoint pathways potentially involved in the transcriptional regulation of *CBR1*, we analyzed the effect of different receptor activators on *CBR1* mRNA levels. Cultures of HepG2 cells were incubated with different receptor activators at concentrations known to affect the regulation of other drug-metabolizing enzymes (Schuetz et al., 1993; Zhang et al., 2003; Hempel et al., 2004). *CBR1* and β-actin (normalizer) mRNA levels were determined simultaneously by quantitative real-time RT-PCR (see *Materials and Methods*). We detected no changes in *CBR1* mRNA levels after incubations with the glucocorticoid receptor agonist dexamethasone. Likewise, incubations with activators of constitutive androstane receptor (clotrimazole and TCPOBOP) and pregnane X receptor (rifampicin) did not significantly affect *CBR1* mRNA levels. In contrast, incubations with the prototypical AHR ligand β-naphthoflavone (50 μM, 24 h) induced *CBR1* mRNA levels by 5.5-fold (Student's t test, $p < 0.005$) compared with controls (Fig. 3). In MCF-7 cells, β-naphthoflavone exerted moderate cytotoxicity (≈20–30%) at the 50 μM concentration, whereas incubations with 10 μM resulted in negligible cytotoxicity (≤ 5%) and induced *CBR1* mRNA by 2.5-fold (Student's t test, $p < 0.05$; Fig. 3). The increase in *CBR1* mRNA levels in MCF-7 cells treated with β-naphthoflavone was paralleled by a 3-fold increase in maximal cytosolic CBR activity ($CBR_{controls\ (DMSO)}$: 50 ± 13 pmol/min · mg versus $CBR_{\beta\text{-naphthoflavone}}$: 140 ± 2 pmol/min · mg).

Transcriptional Activation of *CBR1* Promoter Constructs by β-Naphthoflavone. Next, we tested whether β-naphthoflavone induced the gene reporter activities of different *CBR1* promoter constructs encompassing up to 1561 bp of the 5′ flanking region. In all cases, incubations with β-naphthoflavone (10 μM, 48 h) or vehicle (DMSO) were performed 24 h after the cotransfections with reporter constructs (see *Materials and Methods*). On average, β-naphthoflavone induced the luciferase activities of the constructs by 11-fold ($_{-1561}$*CBR1*, $p < 0.05$), 5-fold ($_{-600}$*CBR1*, $p <$

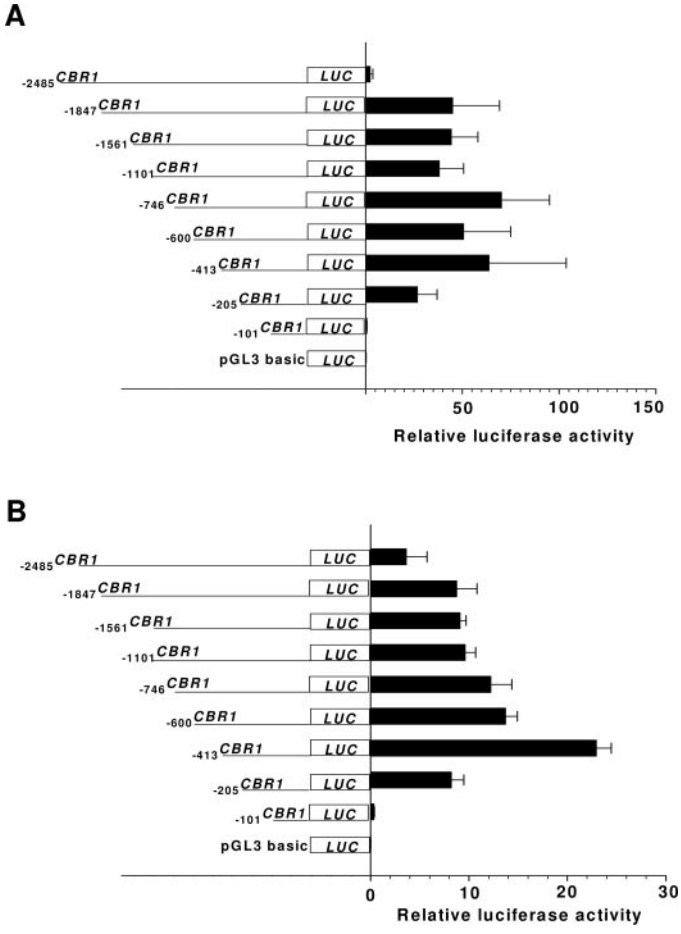

Fig. 2. Functional analysis of human *CBR1* promoter constructs in HepG2 cells (A) and MCF-7 cells (B). Panels show schematic representations of each *CBR1* promoter construct (left) and its corresponding luciferase activity from gene reporter experiments (right). Luciferase activities were measured as described under *Materials and Methods*. Light intensity values from transfections with the promoterless vector were used to correct for background. Corrected luciferase activity values were normalized to *R. reniformis* luciferase activity and expressed as fold increases with respect to the values obtained with pGL3-basic empty vector. Each value represents the mean ± S.D. of four independent experiments performed in duplicate.

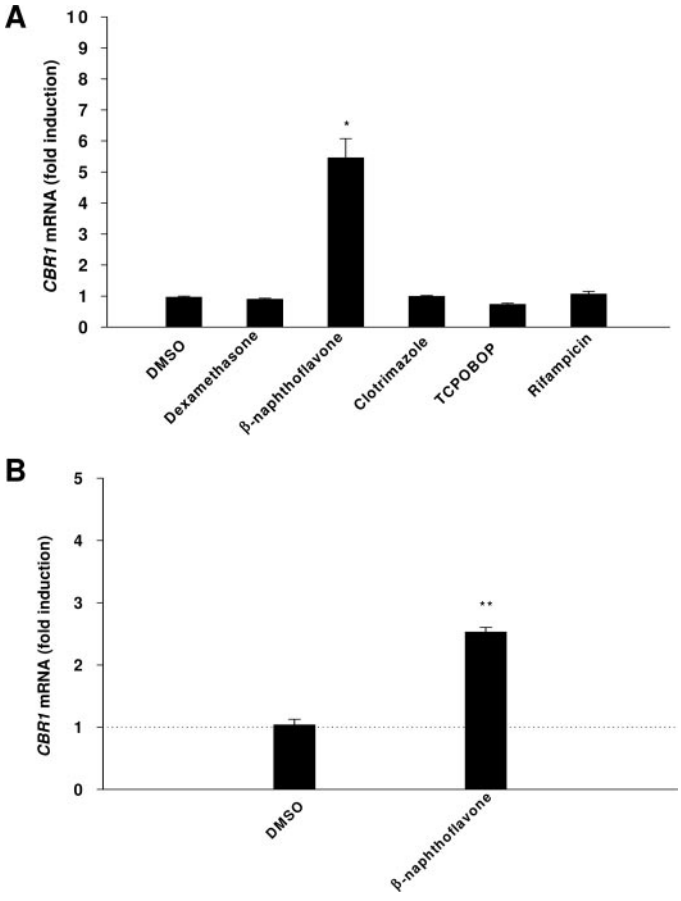

Fig. 3. Induction of *CBR1* mRNA in HepG2 cells (A) and MCF-7 cells (B) by prototypical receptor activators. HepG2 cells were incubated with vehicle (DMSO, 0.01%), dexamethasone (10 μM), β-naphthoflavone (50 μM), clotrimazole (20 μM), TCPOBOP (0.250 μM), and rifampicin (10 μM) for 24 h. MCF-7 cells were incubated with vehicle (DMSO, 0.01%) and β-naphthoflavone (10 μM) for 24 h. The expression of *CBR1* mRNA was analyzed by quantitative real-time RT-PCR using specific primers as described under *Materials and Methods*. Each value represents the mean ± S.D. from three independent experiments analyzed in quadruplicate. Asterisks indicate significant differences from the *CBR1* mRNA levels from vehicle treated cells (*, $p < 0.005$; **, $p < 0.05$).

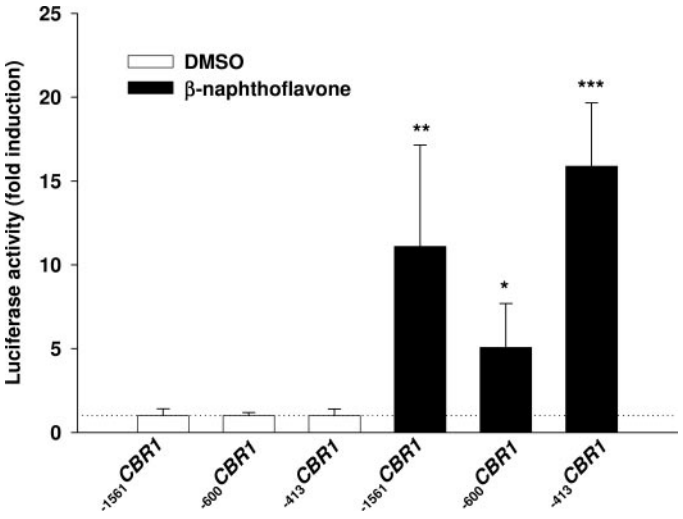

Fig. 4. Effect of the AHR ligand β-naphthoflavone on the gene reporter activities of *CBR1* promoter constructs. Cultures of MCF-7 cells were cotransfected with *CBR1* reporter constructs ($_{-1561}$*CBR1*, $_{-600}$*CBR1*, and $_{-413}$*CBR1*) and the normalizer plasmid pRL-SV40. Twenty-four hours after cotransfections, cells were treated with β-naphthoflavone (10 μM) or vehicle (DMSO, 0.01%) for 48 h. Luciferase activities were measured as described under *Materials and Methods*. For each construct, normalized luciferase activities were expressed as fold increases with respect to the values from control incubations, which were set arbitrarily at 1. Data represent the mean ± S.D. from three independent experiments performed in duplicate. Asterisks indicate significant difference from vehicle-treated cells (*, $p < 0.05$; **, $p < 0.05$; ***, $p < 0.001$).

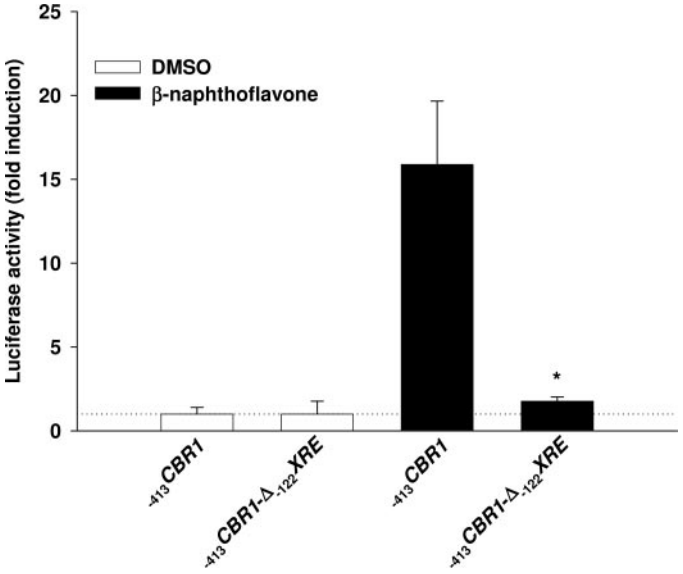

Fig. 5. Effect of β-naphthoflavone on the gene reporter activities of the promoter constructs $_{-413}$*CBR1* and $_{-413}$*CBR1*-Δ$_{-122}$ *XRE*. Cotransfections included the normalizer construct (pRL-SV40) and either the intact $_{-413}$*CBR1* construct or the engineered $_{-413}$*CBR1*-Δ$_{-122}$*XRE* construct (without $_{-122}$*XRE* motif). Twenty-four hours after cotransfections, cells were treated with β-naphthoflavone (10 μM) or vehicle (DMSO, 0.01%) for 48 h. Luciferase activities were measured as described under *Materials and Methods*. For each construct, normalized luciferase activities were expressed as fold increases with respect to the values from control incubations (DMSO), which were set arbitrarily at 1. Data represent the mean ± S.D. from three independent experiments performed in duplicate. The asterisk indicates significant difference from the luciferase activity exerted by the $_{-413}$CBR1 construct in the presence of β-naphthoflavone (*, $p < 0.001$).

0.05), and 15-fold ($_{-413}$*CBR1*, $p < 0.001$) in MCF-7 cells compared with vehicle-treated controls (Fig. 4).

Functional *XRE* motifs in the promoters of drug-metabolizing enzymes are necessary to activate gene transcription in response to AHR ligands (Nioi and Hayes, 2004). Thus, we first we tested whether the $_{-122}$*XRE* motif was necessary to induce luciferase reporter gene expression in the presence of the ligand β-naphthoflavone. The removal of $_{-122}$*XRE* decreased the β-naphthoflavone response by 9-fold in MCF-7 cells (Student's *t* test, $p < 0.001$; Fig. 5).

In another set of experiments, we evaluated the ability of the distal $_{-5783}$*XRE* to augment reporter gene activity in response to β-naphthoflavone. To achieve this end, a 12-bp sequence (bases, −5790 to −5779) containing the $_{-5783}$*XRE* was fused into the $_{-2485}$*CBR1* reporter construct. Treatment with β-naphthoflavone increased the reporter activity of $_{-2485}$*CBR1* by 4-fold compared with incubations with the vehicle DMSO (Student's *t* test, $p < 0.05$). Fusion of the distal $_{-5783}$*XRE* to $_{-2485}$*CBR1* further enhanced the β-naphthoflavone response by 5-fold (Student's *t* test, $p < 0.0001$; Fig. 6).

Induction of Hepatic *Cbr1* by TCDD Treatment in *Ahr*$^{+/-}$ and *Ahr*$^{-/-}$ Mice. We extended our observations by evaluating whether the administration of the potent AHR ligand TCDD affected the expression of *Cbr1* in livers from *Ahr*$^{+/-}$ and *Ahr*$^{-/-}$ mice. First, TCDD (50 μg/kg) was administered by a single intraperitoneal injection, and the expres-

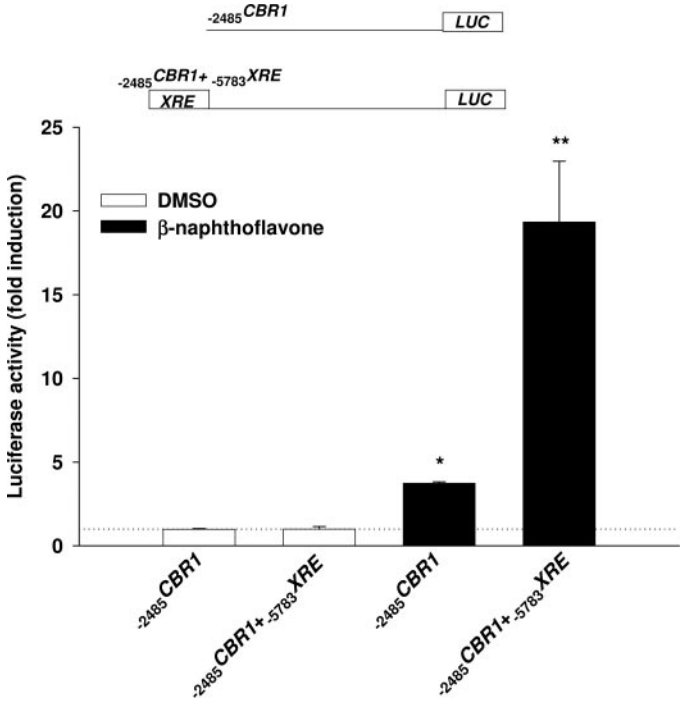

Fig. 6. Effect of β-naphthoflavone on the gene reporter activities of $_{-2485}$*CBR1* and $_{-2485}$*CBR1* + $_{-5783}$*XRE*. Both constructs are schematized at the top of the graph. Cotransfections included the normalizer construct (pRL-SV40) and either the intact $_{-2485}$*CBR1* construct or the engineered $_{-2485}$*CBR1* + $_{-5783}$*XRE* construct. Twenty-four hours after cotransfections, cells were treated with β-naphthoflavone (10 μM) or vehicle (DMSO, 0.01%) for 48 h. Luciferase activities were measured as described under *Materials and Methods*. For each construct, normalized luciferase activities were expressed as fold increases with respect to the values from control incubations, which were set arbitrarily at 1. Data represent the mean ± S.D. from three independent experiments performed in duplicate. Asterisks indicate significant difference from vehicle treated cells (*, $p < 0.05$; **, $p < 0.0001$).

sions of *Cbr1* mRNA and protein were analyzed from livers collected 72 h after treatments. In heterozygous $Ahr^{+/-}$ animals, TCDD treatment resulted in a 2-fold induction of *Cbr1* mRNA levels compared with vehicle-treated heterozygous controls. In contrast, TCDD treatment failed to induce the expression of hepatic *Cbr1* mRNA in homozygous null ($Ahr^{-/-}$) mice (Fig. 7, A and B). It is noteworthy that the induction of hepatic *Cbr1* mRNA in heterozygous $Ahr^{+/-}$ animals treated with TCDD was paralleled by a 2-fold increase in Cbr1 protein levels as determined by semiquantitative immunoblotting (Fig. 7, C–F). In line, hepatic Cbr activity increased by 40% in TCDD-treated mice with one active *Ahr* allele ($Ahr^{+/-}$), whereas the levels of Cbr activity remained essentially unchanged in the livers of TCDD-treated $Ahr^{-/-}$ mice (data not shown). Moreover, Cbr activity was induced by 5-fold in livers of $Ahr^{+/-}$ mice treated with three consecutive doses of TCDD (50 μg/kg/day for 3 days) compared with vehicle-treated animals ($p < 0.05$; Fig. 8A). Identical TCDD treatments failed to induce hepatic Cbr activity in $Ahr^{-/-}$ mice ($p = 0.32$; Fig. 8B).

Discussion

The first aim of our study was to perform the functional characterization of the promoter of human *CBR1*. Our sequence annotation showed that the core promoter of *CBR1* has the features of a prototypical CpG promoter including two GC boxes, proximal SP1 sites, and the absence of TATA and downstream core promoter element elements (Fig. 1). In humans, approximately half of the promoter regions are located in CpG islands, and gene transcription may occur at different start sites (Butler and Kadonaga, 2002). In line, *CBR1* has a predominant start site at −92 bp, and 16% of the clones reported in DBTSS showed alternative start sites (e.g., −101 and −125 bp). Our results from gene reporter experiments in HepG2 and MCF-7 cells demonstrated the presence of regulatory regions that seem to be relevant to promote transcription under basal conditions in both cell types. For example, deletion of the segment that contains the two GC boxes and the proximal $_{-122}$*XRE* (−205/−101) significantly reduced the reporter gene activity of the $_{-205}$*CBR1* construct compared with the $_{-413}$*CBR1* construct in HepG2 (22-fold)

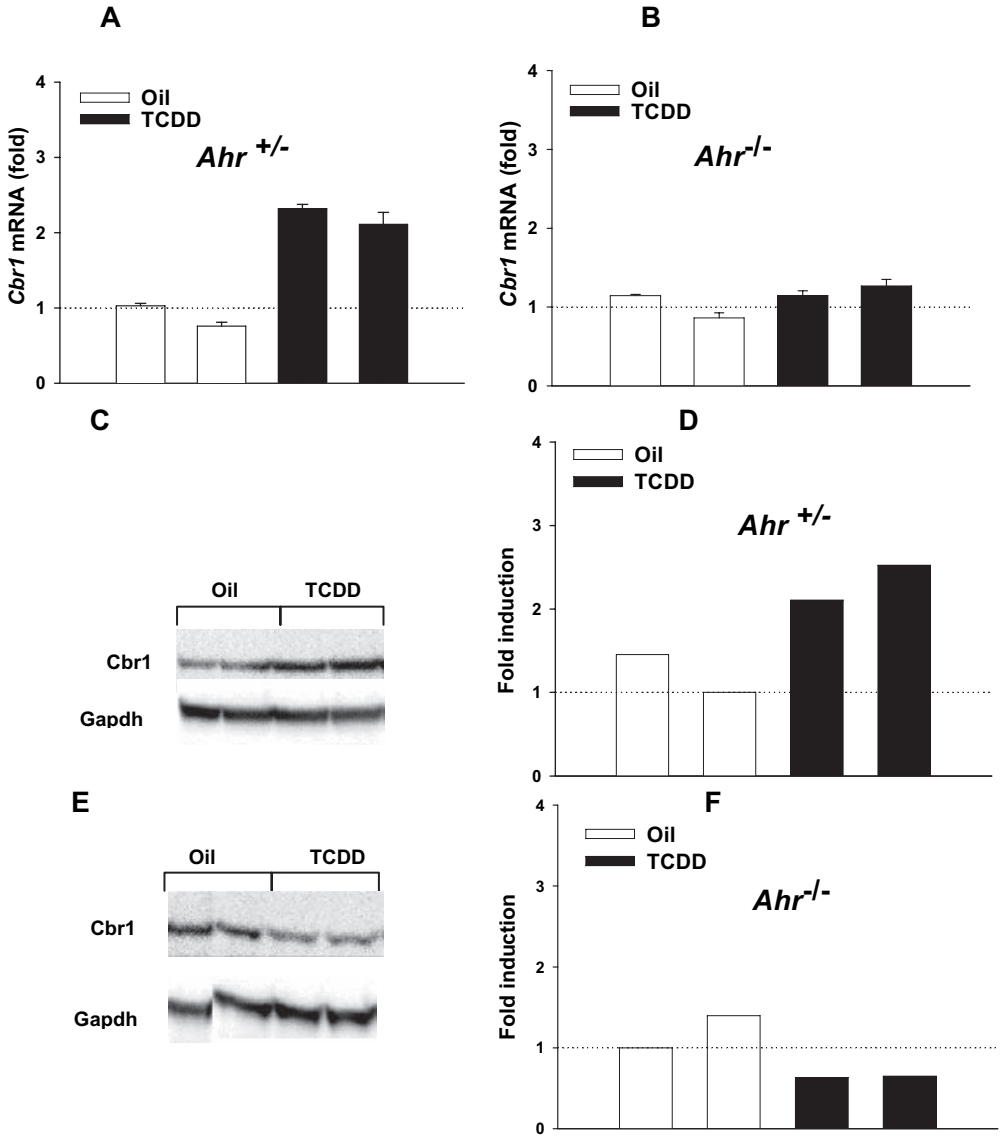

Fig. 7. Effect of TCDD on *Cbr1* mRNA and Cbr1 protein expression in livers from $Ahr^{+/-}$ and $Ahr^{-/-}$ mice. Hepatic *Cbr1* mRNA levels in $Ahr^{+/-}$ (A) and $Ahr^{-/-}$ (B) mice treated with vehicle ($n = 2$) or TCDD ($n = 2$), respectively. The expression of *Cbr1* mRNA was analyzed by using specific primers as described under *Materials and Methods*. Bars represent the mean ± S.D. from two quantifications performed in quadruplicate for each animal. Immunodetection of hepatic Cbr1 in $Ahr^{+/-}$ (C) and $Ahr^{-/-}$ mice (E). Hepatic Cbr1 and GAPDH were detected with specific antibodies as described under *Materials and Methods*. Immunoreactive bands were visualized in a ChemiDoc XRS gel documentation system. The intensities from the immunoreactive GAPDH bands were used to correct for differences in protein loading during densitometric analyses. Densitometric analyses of Cbr1 in livers from $Ahr^{+/-}$ (D) and $Ahr^{-/-}$ mice (F). Each bar represent the level of Cbr1 expressed as fold induction with respect to the average intensity value obtained from vehicle-treated animals.

and MCF-7 (41-fold) cells. It has been demonstrated that SP1 binding sites together with an Inr motif can activate transcription in CpG promoters (Smale and Baltimore, 1989; Butler and Kadonaga, 2002). Consequently, the *CBR1* −101/+1 region harboring both SP1 and Inr consensus displayed minimal although significant promoter activities in both cell lines. Functional mutagenesis analysis within the context of the minimal *CBR1* promoter will provide further evidence on the role of the Inr and SP1 elements.

The second aim of this study was to evaluate the ability of prototypical receptor activators to induce the expression of *CBR1* mRNA. In agreement with the seminal observation by Forrest et al. (1990), the AHR ligand β-naphthoflavone was the only compound that significantly induced *CBR1* mRNA levels in HepG2 and MCF-7 cells. Furthermore, our data with engineered reporter constructs suggest that $_{-122}$*XRE*, and $_{-5697}$*XRE* may act as bona fide functional elements to activate AHR-mediated gene transcription in the presence of AHR ligands.

The overall identity between the human *CBR1* proximal promoter region (≈600 bp) and the mouse *Cbr1* putative promoter region is 33% (global alignment analysis). Similar overall identity values (≈36%) were obtained when comparisons were extended up to 2500 bp. Further analysis by using the sequence comparison tool from DBTSS pinpointed 3 DNA fragments (size range, 38–42 bp) with relatively high sequence identity values (average, 72%). In addition, we identified a proximal *XRE* and a GC box element on the murine sequence that correspond with similar motifs on the human *CBR1* promoter (Fig. 9). Sun et al. (2004) analyzed the positional conservation of *XRE* core motifs between several murine and human genes and found that only 39% of the human-mouse orthologs contain positionally conserved *XREs*. Thus, the positional conservation of the substitution-intolerant *XRE* core in both murine and human *CBR1* sequences is interesting and supports the notion that the transcription of *CBR1* in both species is controlled by similar key regulatory factors (e.g., AHR). Furthermore, our experiments with heterozygous $Ahr^{+/-}$ and homozygous $Ahr^{-/-}$ mice clearly showed that Ahr plays a pivotal role in mediating *Cbr1* induction in vivo. It is noteworthy that the presence of one active *Ahr* allele was essential to induce *Cbr1* mRNA, Cbr1 protein, and Cbr activity in $Ahr^{+/-}$ mice treated with the AHR ligand TCDD. In contrast, TCDD treatment failed to induce *Cbr1* expression in homozygous null animals ($Ahr^{-/-}$).

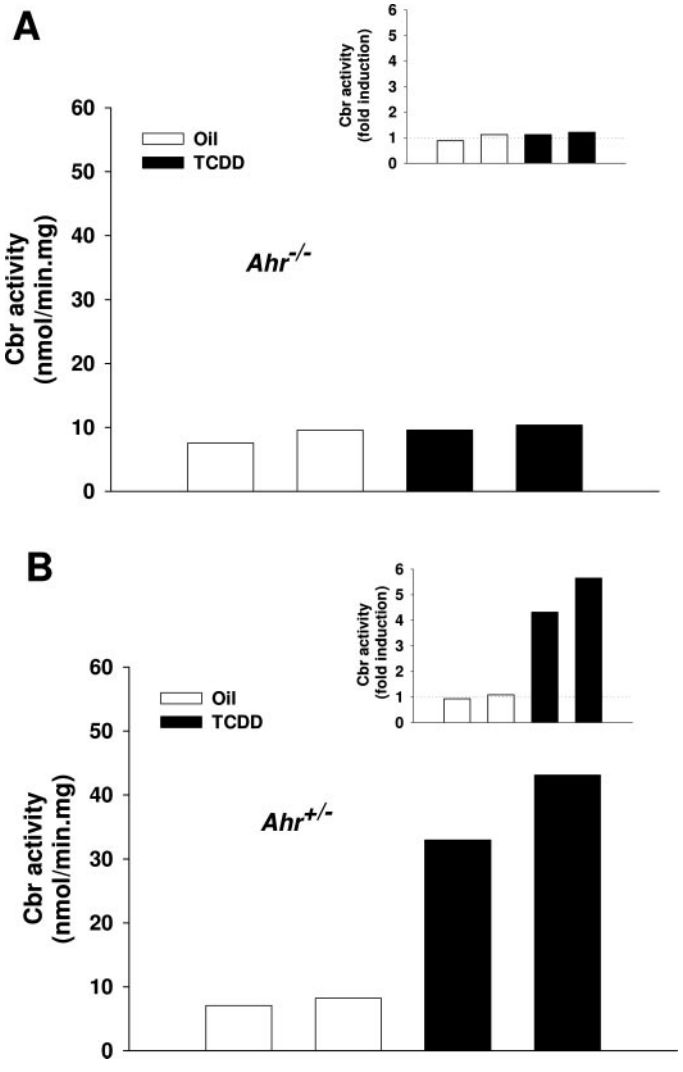

Fig. 8. Effect of TCDD on hepatic Cbr activity in heterozygous $Ahr^{+/-}$ (A) and homozygous $Ahr^{-/-}$ (B) mice. Each bar represents the average from two measurements performed in duplicate. Insets, hepatic Cbr activity expressed as fold induction with respect to the average activity value obtained from vehicle-treated animals.

The reduction of carbonyl moieties catalyzed by CBR1 is an important step in the metabolism of a wide variety of clinically relevant drugs such as the anticancer daunorubicin, the antipsychotic haloperidol, and the antidiabetic acetohexamide (Ohara et al., 1995; Forrest and Gonzalez, 2000; Rosemond and Walsh, 2004). CBR1 also catalyzes the reduction of toxins such as the potent tobacco carcinogen 4-methylnitrosamino-1-(3-pyridyl)-1-butanone (NNK). In humans, NNK is detoxified through two-electron reductions catalyzed mainly by cytosolic CBR1 and microsomal 11β-hydroxysteroid dehydrogenase type I. The resulting alcohol metabolite 4-methylnitrosamino-1-(3-pyridyl)-1-butanol can be further subjected to glucuronidation to form 4-methylnitrosamino-1-(3-pyridyl)-1-butanol-glucuronide, which is excreted in urine (Maser et al., 2000). Variable *CBR1* mRNA expression has been described in human lung, and a recent study on 59 patients with non–small-cell lung carcinoma reported higher postoperative survival rates among patients having tumors containing "high" *CBR1* mRNA expression compared with those with tumors presenting "low" *CBR1* mRNA expression (5-year survival *CBR1*-high, 68.3%, versus 5-year survival *CBR1*-low, 36.5%; $p = 0.03$) (Finckh et al., 2001; Takenaka et al., 2005). The polycyclic aromatic hydrocarbon benzo(*a*)pyrene (BP) is one of the best-characterized carcinogens in cigarette smoke and is also a powerful AHR ligand (Denison and Nagy, 2003). Moreover, BP induces *Cbr1* expression significantly in *Ahr*-proficient mice but fails to induce *Cbr1* in *Ahr*-deficient animals (S. S. Lakhman, E. G. Schuetz, and J. G. Blanco, unpublished observations). Thus, it is reasonable to hypothesize that BP may modulate *CBR1* expression in the lungs of smokers via the AHR pathway, which in turn has an impact on the CBR1-mediated detoxification of other smoke carcinogens relevant to the pathogenesis of lung cancer such as NNK. In conclusion, our results describe the first functional characterization of the promoter of human *CBR1*

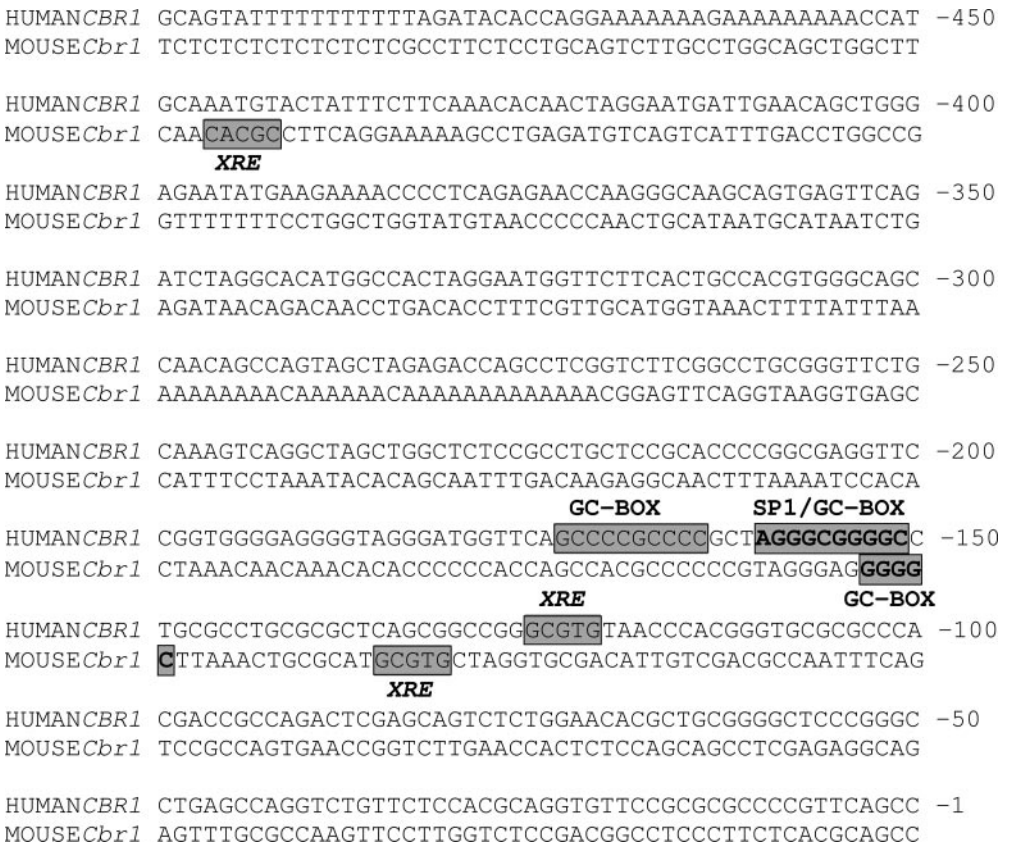

Fig. 9. DNA sequence alignment of the human and mice *CBR1* 5′-flanking regions. Sequences were aligned by using the global positioning alignment algorithm. *XRE* core motifs and GC boxes are highlighted in gray.

and indicate that AHR is a key mediator in dictating variable CBR activity.

Acknowledgments

We gratefully acknowledge the excellent assistance of Dr. Lubin Lan.

References

Bello RI, Gomez-Diaz C, Navas P, and Villalba JM (2004) NAD(P)H:quinone oxidoreductase 1 expression, hydrogen peroxide levels, and growth phase in HeLa cells. *Methods Enzymol* **382:**234–243.

Blanquicett C, Johnson MR, Heslin M, and Diasio RB (2002) Housekeeping gene variability in normal and carcinomatous colorectal and liver tissues: applications in pharmacogenomic gene expression studies. *Anal Biochem* **303:**209–214.

Bustin SA (2002) Quantification of mRNA using real-time reverse transcription PCR (RT-PCR): trends and problems. *J Mol Endocrinol* **29:**23–39.

Butler JEF and Kadonaga JT (2002) The RNA polymerase II core promoter: a key component in the regulation of gene expression. *Genes Dev* **16:**2583–2592.

Covarrubias VG, Lakhman SS, Forrest A, Relling MV, and Blanco JG (2006) Higher activity of polymorphic NAD(P)H:quinone oxidoreductase in liver cytosols from blacks compared to whites. *Toxicol Lett* **164:**249–258.

Denison MS and Nagy SR (2003) Activation of the aryl hydrocarbon receptor by structurally diverse exogenous and endogenous chemicals. *Annu Rev Pharmacol Toxicol* **43:**309–334.

Fernandez-Salguero P, Pineau T, Hilbert DM, McPhail T, Lee SS, Kimura S, Nebert DW, Rudikoff S, Ward JM, and Gonzalez FJ (1995) Immune system impairment and hepatic fibrosis in mice lacking the dioxin-binding Ah receptor. *Science* **268:** 722–726.

Finckh C, Atalla A, Nagel G, Stinner B, and Maser E (2001) Expression and NNK reducing activities of carbonyl reductase and 11beta-hydroxysteroid dehydrogenase type 1 in human lung. *Chem Biol Interact* **130-132:**761–773.

Forrest GL, Akman S, Krutzik S, Paxton RJ, Sparkes RS, Doroshow J, Felsted RL, Glover CJ, Mohandas T, and Bachur NR (1990) Induction of a human carbonyl reductase gene located on chromosome 21. *Biochim Biophys Acta* **1048:**149–155.

Forrest GL and Gonzalez B (2000) Carbonyl reductase. *Chem Biol Interact* **129:**21–40.

Frost BM, Eksborg S, Bjork O, Abrahamsson J, Behrendtz M, Castor A, Forestier E, and Lonnerholm G (2002) Pharmacokinetics of doxorubicin in children with acute lymphoblastic leukemia: multi-institutional collaborative study. *Med Pediatr Oncol* **38:**329–337.

Hempel N, Wang H, LeCluyse EL, McManus ME, and Negishi M (2004) The human sulfotransferase SULT1A1 gene is regulated in a synergistic manner by Sp1 and GA binding protein. *Mol Pharmacol* **66:**1690–1701.

Iwata N, Inazu N, Hara S, Yanase T, Kano S, Endo T, Kuriiwa F, Sato Y, and Satoh T (1993) Interindividual variability of carbonyl reductase levels in human livers. *Biochem Pharmacol* **45:**1711–1714.

Jiang W, Welty SE, Couroucli XI, Barrios R, Kondraganti SR, Muthiah K, Yu L, Avery SE, and Moorthy B (2004) Disruption of the Ah receptor gene alters the susceptibility of mice to oxygen-mediated regulation of pulmonary and hepatic cytochromes P4501A expression and exacerbates hyperoxic lung injury. *J Pharmacol Exp Ther* **310:**512–519.

Lopez de Cerain A, Marin A, Idoate MA, Tunon MT, and Bello J (1999) Carbonyl reductase and NADPH cytochrome P450 reductase activities in human tumoral versus normal tissues. *Eur J Cancer* **35:**320–324.

Lusska A, Shen E, and Whitlock JP Jr (1993) Protein-DNA interactions at a dioxin-responsive enhancer. Analysis of six bona fide DNA-binding sites for the liganded Ah receptor. *J Biol Chem* **268:**6575–6580.

Maser E, Stinner B, and Atalla A (2000) Carbonyl reduction of 4-(methylnitrosamino)-1-(3-pyridyl)-1-butanone (NNK) by cytosolic enzymes in human liver and lung. *Cancer Lett* **148:**135–144.

Minotti G, Menna P, Salvatorelli E, Cairo G, and Gianni L (2004) Anthracyclines: molecular advances and pharmacologic developments in antitumor activity and cardiotoxicity. *Pharmacol Rev* **56:**185–229.

Nebert DW, Roe AL, Dieter MZ, Solis WA, Yang Y, and Dalton TP (2000) Role of the aromatic hydrocarbon receptor and [Ah] gene battery in the oxidative stress response, cell cycle control, and apoptosis. *Biochem Pharmacol* **59:**65–85.

Nioi P and Hayes JD (2004) Contribution of NAD(P)H:quinone oxidoreductase 1 to protection against carcinogenesis, and regulation of its gene by the Nrf2 basic-region leucine zipper and the arylhydrocarbon receptor basic helix-loop-helix transcription factors. *Mutat Res* **555:**149–171.

Ohara H, Miyabe Y, Deyashiki Y, Matsuura K, and Hara A (1995) Reduction of drug ketones by dihydrodiol dehydrogenases, carbonyl reductase and aldehyde reductase of human liver. *Biochem Pharmacol* **50:**221–227.

Rady-Pentek P, Mueller R, Tang BK, and Kalow W (1997) Interindividual variation in the enzymatic 15-keto-reduction of 13,14-dihydro-15-keto-prostaglandin E1 in human liver and in human erythrocytes. *Eur J Clin Pharmacol* **52:**147–153.

Rosemond MJ and Walsh JS (2004) Human carbonyl reduction pathways and a strategy for their study in vitro. *Drug Metab Rev* **36:**335–361.

Schuetz EG, Schuetz JD, Strom SC, Thompson MT, Fisher RA, Molowa DT, Li D, and Guzelian PS (1993) Regulation of human liver cytochromes P-450 in family 3A in primary and continuous culture of human hepatocytes. *Hepatology* **18:**1254–1262.

Shimada T, Inoue K, Suzuki Y, Kawai T, Azuma E, Nakajima T, Shindo M, Kurose K, Sugie A, Yamagishi Y, et al. (2002) Arylhydrocarbon receptor-dependent induction of liver and lung cytochromes P450 1A1, 1A2, and 1B1 by polycyclic aromatic hydrocarbons and polychlorinated biphenyls in genetically engineered C57BL/6J mice. *Carcinogenesis* **23:**1199–1207.

Smale ST and Baltimore D (1989) The "initiator" as a transcription control element. *Cell* **57:**103–113.

Sugihara K, Kitamura S, Yamada T, Ohta S, Yamashita K, Yasuda M, and Fujii-Kuriyama Y (2001) Aryl hydrocarbon receptor (AhR)-mediated induction of xan-

thine oxidase/xanthine dehydrogenase activity by 2,3,7,8-tetrachlorodibenzo-p-dioxin. *Biochem Biophys Res Commun* **281:**1093–1099.
Sun YV, Boverhof DR, Burgoon LD, Fielden MR, and Zacharewski TR (2004) Comparative analysis of dioxin response elements in human, mouse and rat genomic sequences. *Nucleic Acids Res* **32:**4512–4523.
Takenaka K, Ogawa E, Oyanagi H, Wada H, and Tanaka F (2005) Carbonyl reductase expression and its clinical significance in non-small-cell lung cancer. *Cancer Epidemiol Biomarkers Prev* **14:**1972–1975.
Wermuth B, Bohren KM, Heinemann G, von Wartburg JP, and Gabbay KH (1988) Human carbonyl reductase. Nucleotide sequence analysis of a cDNA and amino acid sequence of the encoded protein. *J Biol Chem* **263:**16185–16188.
Wermuth B, Platts KL, Seidel A, and Oesch F (1986) Carbonyl reductase provides the enzymatic basis of quinone detoxication in man. *Biochem Pharmacol* **35:**1277–1282.
Wong JM, Kalow W, Kadar D, Takamatsu Y, and Inaba T (1993) Carbonyl (phenone) reductase in human liver: inter-individual variability. *Pharmacogenetics* **3:**110–115.
Zaher H, Yang TJ, Gelboin HV, Fernandez-Salguero P, and Gonzalez FJ (1998) Effect of phenobarbital on hepatic CYP1A1 and CYP1A2 in the Ahr-null mouse. *Biochem Pharmacol* **55:**235–238.
Zhang S, Qin C, and Safe SH (2003) Flavonoids as aryl hydrocarbon receptor agonists/antagonists: effects of structure and cell context. *Environ Health Perspect* **111:**1877–1882.

Address correspondence to: Dr. Javier G. Blanco, 545 Cooke Hall, Department of Pharmaceutical Sciences, The State University of New York at Buffalo, Buffalo, NY 14260-1200. E-mail: jgblanco@buffalo.edu